

RESEARCH ARTICLE

Open Access

Heterogeneity analysis of the proteomes in clinically nonfunctional pituitary adenomas

Xianquan Zhan^{1,2,3,4*}, Xiaowei Wang^{1,2,3}, Ying Long^{1,2,3} and Dominic M Desiderio⁵

Abstract

Background: Clinically nonfunctional pituitary adenomas (NFPAs) without any clinical elevation of hormone and with a difficulty in its early-stage diagnosis are highly heterogeneous with different hormone expressions in NFPA tissues, including luteinizing hormone (LH)-positive, follicle-stimulating hormone (FSH)-positive, LH/FSH-positive, and negative (NF). Elucidation of molecular mechanisms and discovery of biomarkers common and specific to those different subtypes of NFPAs will benefit NFPA patients in early-stage diagnosis and individualized treatment.

Methods: Two-dimensional gel electrophoresis (2DGE) and PDQuest image analyses were used to compare proteomes of different NFPA subtypes (NF-, LH-, FSH-, and LH/FSH-positive) relative to control pituitaries (Con). Differentially expressed proteins (DEPs) were characterized with mass spectrometry (MS). Each set of DEPs in four NFPA subtypes was evaluated with overlap analysis and signaling pathway network analysis with comparison to determine any DEP and pathway network that are common and specific to each NFPA subtype.

Results: A total of 93 differential protein-spots were determined with comparison of each NFPA type (NF-, LH-, FSH-, and LH/FSH-positive) versus control pituitaries. A total of 76 protein-spots were MS-identified (59 DEPs in NF vs. Con; 65 DEPs in LH vs. Con; 63 DEPs in FSH vs. Con; and 55 DEPs in LH/FSH vs. Con). A set of DEPs and pathway network data were common and specific to each NFPA subtype. Four important common pathway systems included MAPK-signaling abnormality, oxidative stress, mitochondrial dysfunction, and cell-cycle dysregulation. However, these pathway systems were, in fact, different among four NFPA subtypes with different protein-expression levels of most of nodes, different protein profiles, and different pathway network profiles.

Conclusions: These result data demonstrate that common and specific DEPs and pathway networks exist in four NFPA subtypes, and clarify proteome heterogeneity of four NFPA subtypes. Those findings will help to elucidate molecular mechanisms of NFPAs, and discover protein biomarkers to effectively manage NFPA patients towards personalized medicine.

Keywords: Nonfunctional pituitary adenoma, Proteome, Heterogeneity, Two-dimensional gel electrophoresis, Mass spectrometry, Differentially expressed protein, Pathway network

Background

Clinically nonfunctional pituitary adenomas (NFPAs) are a very challenging clinical problem in pituitary tumor patients relative to functional pituitary adenomas (FPAs) because an NFPA does not have any elevation of the corresponding hormone [1,2]. Thus, an NFPA commonly

cannot be diagnosed until presentation of visual injuries and compression symptoms of neighboring tissues, when the tumor has progressed to the middle/late stage. An opportunity is lost for early-stage treatment, and central endocrine regulatory roles of the pituitary, are both lost. The use of proteomics to elucidate molecular mechanisms and discover tumor-related NFPA biomarkers is our long-term goal. Extensive proteomics studies of pituitary adenomas have been carried out in our, and other, research groups [3-10], including protein expression profiles [11-14], differentially expressed proteins (DEPs) [15,16], protein post-translational modifications

* Correspondence: yjzhan2011@gmail.com

¹Key Laboratory of Cancer Proteomics of Chinese Ministry of Health, Xiangya Hospital, Central South University, 87 Xiangya Road, Changsha, Hunan 410008, P. R. China

²Hunan Engineering Laboratory for Structural Biology and Drug Design, Xiangya Hospital, Central South University, 87 Xiangya Road, Changsha, Hunan 410008, P. R. China

Full list of author information is available at the end of the article

(PTMs) that include tyrosine nitration [17-19] and phosphorylation [20,21], hormone isoforms [22], protein molecular pathway networks [16,23] from comparative proteomics and systems biology analyses between NFPA versus control tissues [15,23] and between invasive versus noninvasive NFPA [16], and serum protein biomarkers in pituitary adenomas [6-8]. Moreover, a protein antibody array ($n = 1,005$ proteins) based on pituitary adenoma proteomics data was used to analyze human pituitary adenomas and identify a DEP profile [24]. A clinical proteomic method that was used to accurately stratify pituitary adenomas was based on multiplex immunoassays of peptide hormones extracted from formalin-fixed and paraffin-embedded tissue [9,10]. Laser capture microdissection (LCM) coupled with proteomics was used to accurately identify the proteomic variation of an adenoma relative to control pituitary [25-27]. Proteomics data-based systems pathway network analysis revealed four important signal pathway network variations in NFPA pathophysiological processes, including mitochondrial dysfunction, oxidative stress, cell-cycle dysregulation, and MAPK-signaling system abnormality [23]. However, those proteomic studies did not consider NFPA heterogeneity. In fact, NFPA is highly heterogeneous – it has different types of cell origins and hormones expressed in tumor tissues, including silent somatotroph (growth hormone GH-positive; 3%), silent corticotroph (adrenocorticotrophic hormone ACTH-positive; 8%), oncocytoma (no hormone expression; 6%), null cell (no hormone expression; 17%), and gonadotroph (intact follicle-stimulating hormone/luteinizing hormone FSH/LH or subunits; 40-79%) that was subclassified as LH-positive, FSH-positive, and LH/FSH-positive NFPA [15]. Studies demonstrate that the silent hormone expression in NFPA tissue is associated with tumor behaviors such as invasion [28,29]. Therefore, it is essential to investigate proteomic variations in different NFPA subtypes for an in-depth and accurate understanding of common and specific NFPA mechanisms and discovery of reliable biomarkers toward individualized medical practice. Thus, we emphasize the scientific importance to investigate the heterogeneity of NFPA proteomes. A comparative analysis of proteomes in different NFPA subtypes (NF-, LH-, FSH-, and LH/FSH-positive) relative to normal control pituitaries described here revealed variations in protein expressions and pathway networks among four NFPA subtypes, and revealed the common and specific molecular mechanisms and protein biomarkers for different NFPA subtypes.

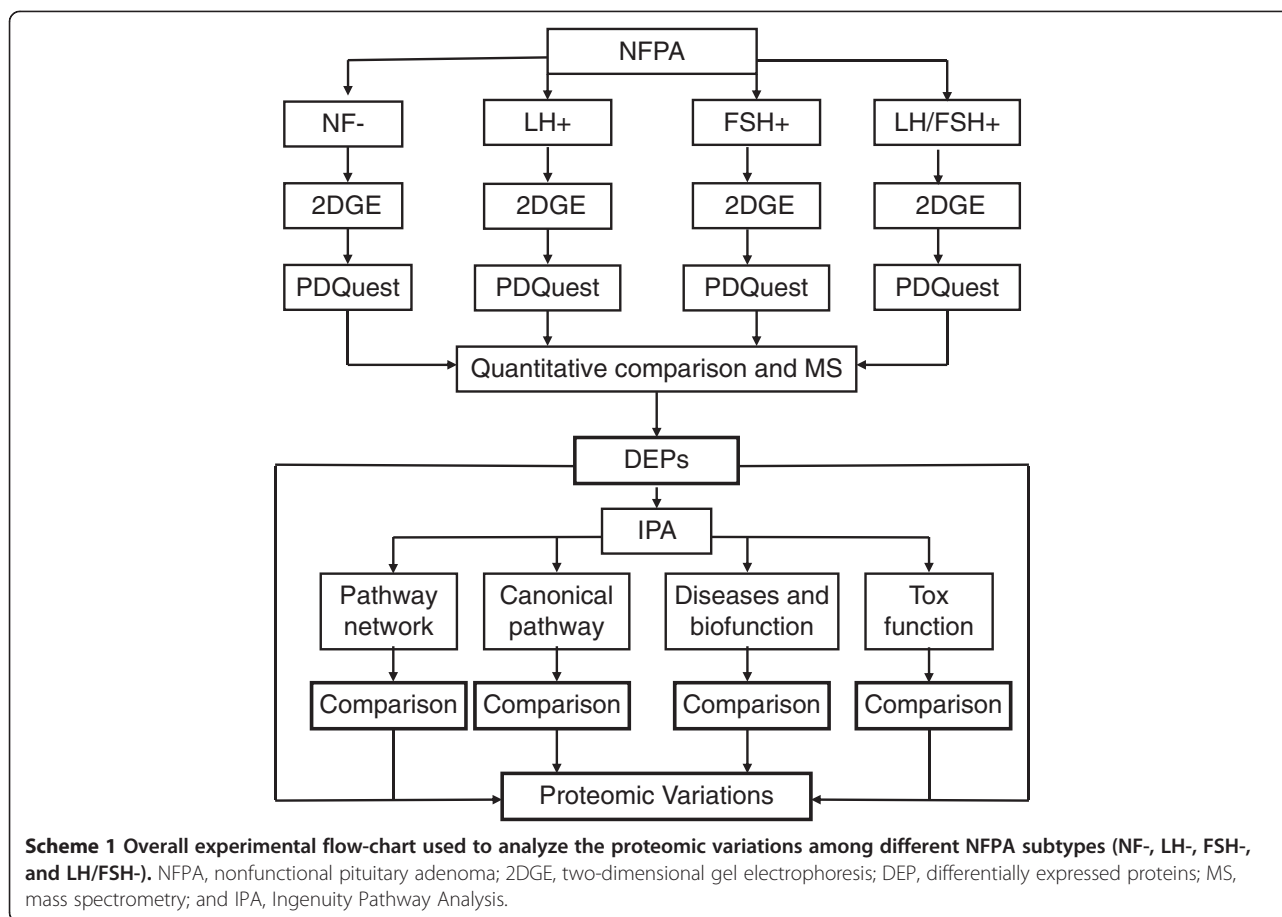
Two-dimensional gel electrophoresis (2DGE)-based comparative proteomics [30,31] is a classical and effective approach to quantify each DEP in different NFPA subtypes (NF-, LH-, FSH-, and LH/FSH-positive) versus normal control pituitaries. The linear dynamic separation range, spatial and quantitative reproducibility, and experimental

conditions of 2DGE-based proteomics were optimized in our previous studies [32,33]. Isoelectric focusing (IEF) has a high reproducibility due to use of highly reproducible commercial immobilized pH gradient (IPG) strip. The vertical multi-gel sodium dodecyl sulfate–polyacrylamide gel electrophoresis (SDS-PAGE) system, which has a higher reproducibility and wider linear dynamic range, was used to array the proteome of each NFPA subtype and control pituitary. PDQuest 2D image software was used to quantify DEPs of each NFPA subtype relative to controls. Matrix-assisted laser desorption/ionization time-of-flight (MALDI-TOF)-based peptide mass fingerprint (PMF), liquid chromatography (LC)-electrospray ionization (ESI)-based tandem mass spectrometry (MS/MS), and human Swiss-Prot protein databases were used to identify each DEP. Systems biology-based pathway network analysis was used to reveal variations of protein molecular networks among different NFPA subtypes. Thus, this study is the first to reveal variations in proteomes and molecular networks among four NFPA subtypes (NF-, LH-, FSH-, LH/FSH-positive NFPA), and the heterogeneity of NFPA proteomes. Scheme 1 shows the overall experimental flowchart that was used to identify variations of proteomes and molecular networks among four NFPA subtypes.

Results

2DGE pattern and DEP profile of each NFPA subtype relative to control pituitaries

2DGE-based comparative proteomics was used to analyze proteome variations from controls ($n = 8$; 3 to 5 gel images per sample) versus each NFPA type, including NF- ($n = 3$; 3 gel images per sample), LH- ($n = 3$; 3 gel images per sample), FSH- ($n = 3$; 3 gel images per sample), and LH/FSH- ($n = 3$; 3 gel images per sample) adenoma tissues. Each sample was 2DGE-analyzed three to five times to provide a triplicate, high-quality 2DGE gel image for each sample. Figure 1 shows the digitized master 2D gel image. *Ca.* 1,000 protein-spots were detected in each gel image with PDQuest 2D gel-image analysis with high-resolution, high-spatial reproducibility in the IEF and SDS-PAGE directions, and high reproducibility for triplicate 2D gel images of each sample. 2DGE protein-spots mainly distributed within pH 4–9 and relative mass (M_r) 15–150 kDa. For each sample, the average between-gel matched percentage ranged from 85% to 99% for control pituitaries and 81% to 90% for NFPA; the positional deviation of matched spots among triplicate 2D gel images was 2.13 ± 0.79 mm in the IEF direction and 1.82 ± 0.68 mm in the SDS-PAGE direction; and the correlation coefficient (r) of normalized spot-volumes for between-gel matched spots was > 0.76 with a range of 0.76-0.92. The high-spatial reproducibility and quantitative reproducibility resulted from the same experimental condition maintained for



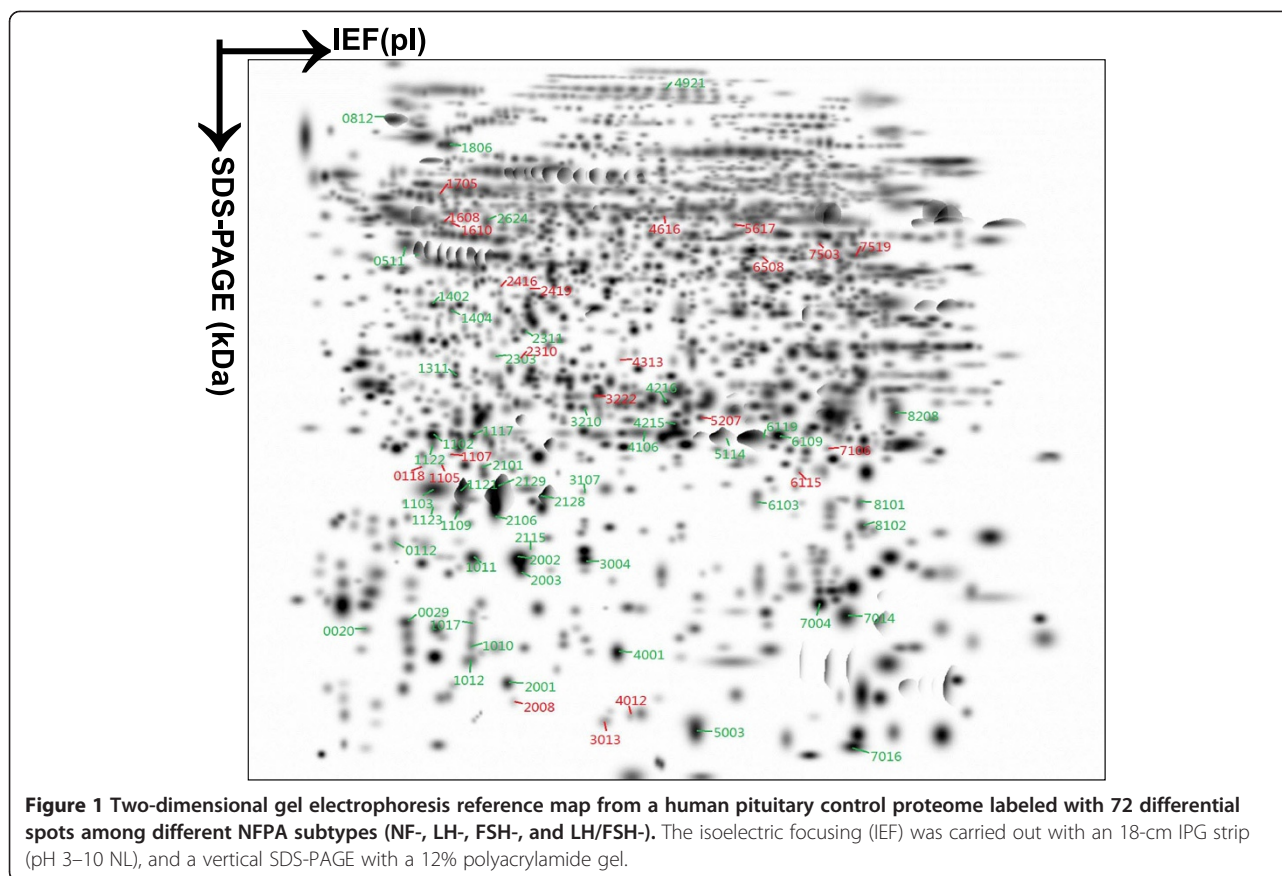
each sample analysis, including sample preparation, IEF, SDS-PAGE, visualization, gel digitalization, and image analysis. That reproducibility provided an accurate comparison between each NFPA subtype and controls.

A total of 93 differential protein-spots was determined with comparison of each NFPA subtype (NF-, LH-, FSH-, and LH/FSH-) versus control pituitaries with a cut-off value of >3-fold and a statistically significant difference ($p < 0.001$). Figure 2 shows a representative DEP-spot (Spot-1311) among different NFPA subtypes ($n = 9$ gel images for each type of NFPAs) versus controls ($n = 30$ gel images) (Figure 2A) and a quantitative comparison of normalized spot-volumes between each NFPA subtype versus controls ($p < 0.001$) (Figure 2B). Each differential protein-spot was labeled in the master gel image (Figure 1). Each differential protein-spot was excised, and proteins were subjected to in-gel digestion with trypsin, followed by MS analysis, including MALDI-TOF PMF and LC-ESI-MS/MS. A total of 72 differential protein-spots that contained DEPs were MS-identified from those 93 differential protein-spots. Four spots (SSP No. 1017, 1103, 2310, and 2419 in Table 1 and Figure 3) of 72 MS-identified spots contained two proteins; therefore, 72 spots represent 76 protein-spots. Among those 76 protein-spots, 59 DEPs

(44 downregulated and 15 upregulated) were identified in NF-NFPA relative to controls, 65 DEPs (45 downregulated and 20 upregulated) in LH-NFPA, 63 DEPs (43 downregulated and 20 upregulated) in FSH-NFPA, and 55 DEPs (41 downregulated and 14 upregulated) in LH/FSH-NFPA. Those DEPs are summarized in Table 1, which contains the SSP number that corresponds to the number labeled in Figure 1, protein name, Swiss-Prot accession number, and fold-value in each NFPA subtype versus controls.

Comparative analysis of DEP profiles derived from four NFPA subtypes relative to controls

An overlapping analysis (Figure 3) among 59 DEPs in NF-NFPA, 65 DEPs in LH-NFPA, 63 DEPs in FSH-NFPA, and 55 DEPs in LH/FSH-NFPA relative to controls (Table 1) revealed that 44 DEPs were common to four NFPA subtypes (NF-, LH-, FSH-, and LH/FSH-). Those 44 common DEP-spots among four NFPA subtypes (NF-, LH-, FSH-, and LH/FSH-) include ten upregulated and 34 downregulated DEPs. Those ten common upregulated DEPs were F-actin capping protein beta unit, splice isoform 2 of F-actin capping protein beta unit, zinc finger protein 266, G(O)-protein alpha subunit 1, G(O)-protein alpha subunit 2, aldose reductase, tryptophan 5-hydroxylase, glutathione



S-transferase Mu-2, isocitrate dehydrogenase [NADP] cytoplasmic, and peroxisomal acyl-coenzyme A thioester hydrolase 2A. The 34 common down-regulated DEPs were somatotropin chain 1, splice isoform 2 of somatotropin precursor, growth hormone variant precursor, prolactin chain 1, splice isoform IL15-S21AA of interleukin-15 precursor, factor X light chain, cytokeratin 16, alpha crystalline C chain, 14-3-3 protein tau, secretagogin, Mu-crystallin homolog, MIMECAN chain 1, tissue transglutaminase, ATP binding protein associated with cell differentiation, N6-adenosine-methyltransferase 70 kDa subunit, hemoglobin beta unit variant, hemoglobin beta-2 chain, and insulin-like growth factor binding. Among them, 16 common DEP-spots contained somatotropin and its isoforms with different *pI* and *M_r*, and four common DEPs contained prolactin and its isoforms with different *pI* and *M_r*. Those common DEPs hint at the common molecular mechanisms and signaling pathways involved in four NFPA subtypes.

Four DEPs (SSP 2101, 4215, 2624, and 1608) were common to only three NFPA subtypes (NF-, LH-, and LH/FSH-), including three down-regulated proteins (somatotropin chain 1, prolactin precursor, and dipeptidyl-peptidase II) and one up-regulated protein (mitochondrial ATP synthase beta chain). Three DEP-spots (SSP 4216,

8102, and 1105) were common to only three NFPA subtypes (LH-, FSH-, and LH/FSH-), including two down-regulated proteins (prolactin chain 1, and phospholipid hydroperoxide glutathione peroxidase) and one up-regulated protein (lactoylglutathione lyase). Two DEP-spots (SSP 2001, and 7106) were common to only three NFPA subtypes (NF-, FSH-, and LH/FSH-), including one down-regulated protein (CD59 glycoprotein) and one up-regulated protein (40 kDa peptidyl-prolyl cis-trans isomerase).

Eight DEPs (SSP 4921, 8208, 0118, 1107, 2008, 3013, 4012, and 6115) were common to only two NFPA subtypes (LH-, and FSH-), including two down-regulated proteins (collagen alpha 2 VI chain, and Ig kappa chain V-III region SIE) and six up-regulated proteins (lactoylglutathione lyase, NADH-ubiquinone oxidoreductase 23 kDa, enhancer of rudimentary homolog, acyl-CoA-binding protein, cytochrome c oxidase polypeptide VIb, and neuronal protein NP25). Four DEPs (SSP 0812, 5003, 1610, and 1705) were common to only two NFPA subtypes (NF-, and LH-), including two down-regulated proteins (tumor rejection antigen 1, and hemoglobin beta-2 chain) and two up-regulated proteins (vimentin, and Rab GDP dissociation). Three DEPs (SSP 2303, 3210, and 5617) were common to only two NFPA subtypes (NF-, and FSH-),

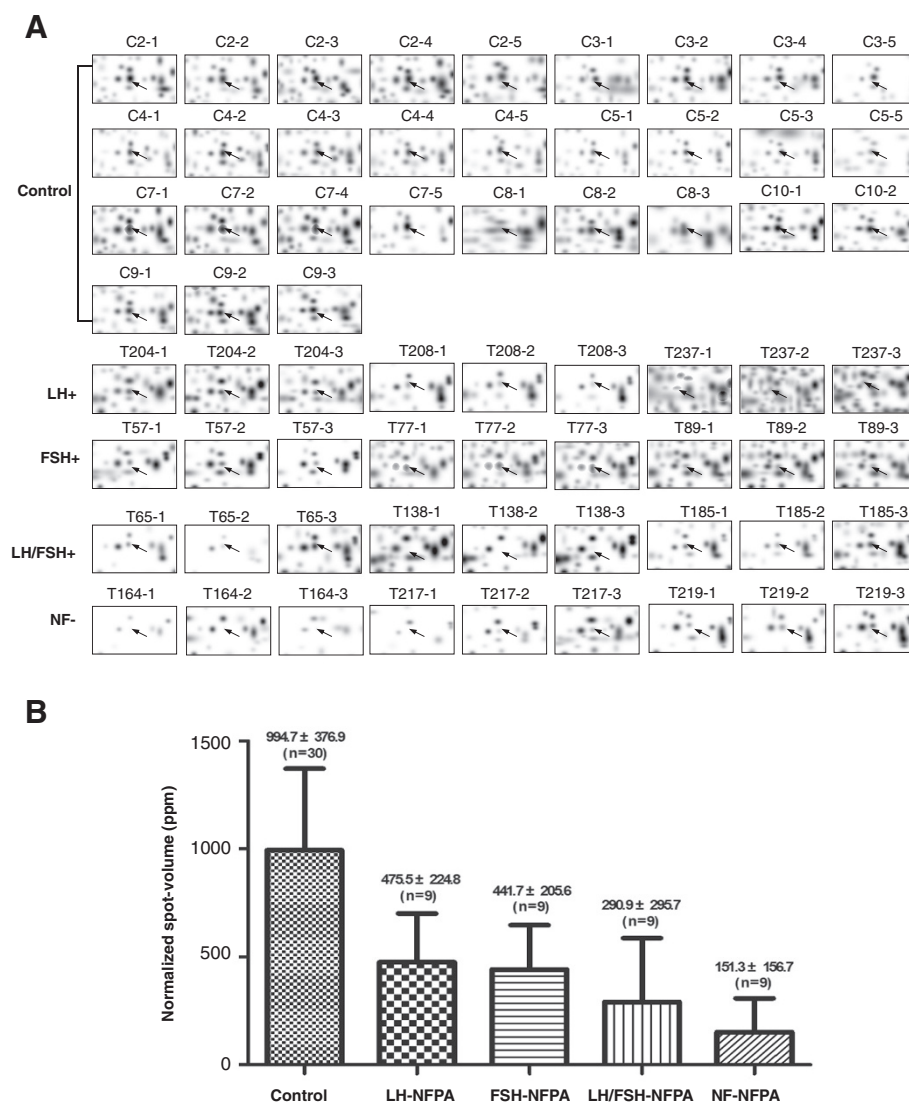


Figure 2 **A** representative differential spot among different NFPA subtypes versus control pituitaries (Spot-1311). Control means control pituitaries; LH means LH-positive NFPA; FSH means FSH-positive NFPA; LH/FSH means LH/FSH-positive NFPA; and NF means NFPA with negative hormone expression. A statistically significant difference existed between each type of NFPA versus control pituitaries ($p < 0.001$). **A**. The 2DGE images (Spot-1311) among four NFPA subtypes. **B**. The normalized spot-volume (Spot-1311) among four NFPA subtypes.

including two down-regulated proteins (serine/threonine protein phosphatase 2A - 55 kDa regulatory subunit B alpha isoform, and heat shock protein 27) and one up-regulated protein (proto-oncogene tyrosine-protein kinase FYN). One DEP-spot (SSP 7016) was common to only two NFPA subtypes (FSH-, and LH/FSH-), which was a down-regulated protein (hemoglobin alpha-2 chain).

Two DEPs (SSP 1012, and 1117) were specific to NF-NFPAs, which were two down-regulated proteins (splice isoform 3 of alpha-s1 casein precursor, and apolipoprotein A-I). Two DEPs (SSP 2311, and 3222) were specific to FSH-NFPAs, including one down-regulated protein (L-Myc-1 protooncogene protein) and one up-regulated protein (endoplasmic reticulum protein ERP29). One

DEP-spot (SSP 1017) was specific to LH-NFPAs, which contained two down-regulated proteins (somatotropin, and splice isoform 2 of somatotropin precursor). One DEP-spot (SSP 7519) was specific to LH/FSH-NFPAs, which was one up-regulated protein (matrix metalloproteinase-19).

Variations in signaling pathway networks among four NFPA subtypes

Each protein functions in an organized, systematic, and dynamic pathway network system. The Ingenuity Pathway Analysis (IPA) program was used to clarify pathway networks that involve each DEP and to address potential biological functions of those DEPs in each NFPA subtype (NF-, LH-, FSH-, and LH/FSH-). DEPs were analyzed with

Table 1 Differentially expressed proteins in different subtypes of clinically nonfunctional pituitary adenomas versus controls

SSP no.	Protein name	Swiss-Prot no.	NF-NFPA	LH-NFPA	FSH-NFPA	LH/FSH-NFPA
1011	Chain 1: somatotropin	P01241	180.6(-)	44.1(-)	82.6(-)	90.5(-)
1017	Chain 1: somatotropin	P01241		13.3(-)		
1017	Splice isoform 2 of somatotropin precursor	P01241 isoform		13.3(-)		
1102	Chain 1: somatotropin	P01241	20.2(-)	6.5(-)	9.1(-)	9.3(-)
1103	Somatotropin precursor	P01241	14.1(-)	2.9(-)	3.3(-)	5.8(-)
1103	Growth hormone variant precursor	P01242	14.1(-)	2.9(-)	3.3(-)	5.8(-)
1109	Chain 1: somatotropin	P01241 isoform	(--)	128.3(-)	69.4(-)	(--)
1121	Chain 1: somatotropin	P01241	6.2(-)	2.8(-)	2.7(-)	3.3(-)
1122	Chain 1: somatotropin	P01241	48.1(-)	(--)	7.5(-)	8.1(-)
1123	Chain 1: somatotropin	P01241	17.3(-)	4.4(-)	6.4(-)	(--)
2002	Splice isoform 2 of somatotropin precursor	P01241 isoform	9.7(-)	3.9(-)	3.2(-)	5.4(-)
2003	Chain 1: somatotropin	P01241	(--)	88.8(-)	25.0(-)	(--)
2101	Chain 1: somatotropin	P01241	27.8(-)	(--)		17.4(-)
2106	Chain 1: somatotropin	P01241	(--)	9.4(-)	2.2(-)	51.2(-)
2115	Chain 1: somatotropin	P01241	(--)	32.1(-)	(--)	(--)
2128	Chain 1: somatotropin	P01241	(--)	82.1(-)	67.4(-)	478.6(-)
2129	Chain 1: somatotropin	P01241	13.4(-)	6.7(-)	4.3(-)	5.5(-)
3004	Chain 1: somatotropin	P01241	42.0(-)	37.0(-)	21.2(-)	13.6(-)
3107	Chain 1: somatotropin	P01241	30.5(-)	(--)	19.1(-)	34.9(-)
4106	Chain 1: prolactin	P01236	8.3(-)	12.6(-)	46.2(-)	99.9(-)
4215	Prolactin precursor	P01236	4.9(-)	4.1(-)		3.8(-)
4216	Chain 1: prolactin	P01236		26.2(-)	14.6(-)	12.3(-)
5114	Chain 1: prolactin	P01236	(--)	20.1(-)	17.6(-)	19.0(-)
6109	Chain 1: prolactin	P01236	(--)	36.7(-)	(--)	19.7(-)
6119	Chain 1: prolactin	P01236	(--)	33.6(-)	11.3(-)	32.6(-)
0020	Splice isoform IL15-S21AA of interleukin-15 precursor	P40933-2 isoform	(--)	(--)	1.6(-)	2.7(-)
0029	Chain 1: Factor X light chain	P00742	(--)	(--)	29.3(-)	38.9(-)
0511	Cytokeratin 16	P08779	28.8(-)	2.1(-)	15.7(-)	18.5(-)
0112	Alpha crystallin C chain	Q9UJY1	(--)	2.3(-)	(--)	(--)
0812	Chain 1: Endoplasmin (Tumor rejection antigen 1)	P14625	11.0(-)	4.4(-)		
1010	14-3-3 protein tau	P27348	(--)	(--)	6.4(-)	15.5(-)
1012	Splice isoform 3 of alpha-s1 casein precursor	P47710-3 isoform	17.8(-)			
1117	Chain 1: apolipoprotein A-I	P02647	2.1(-)			

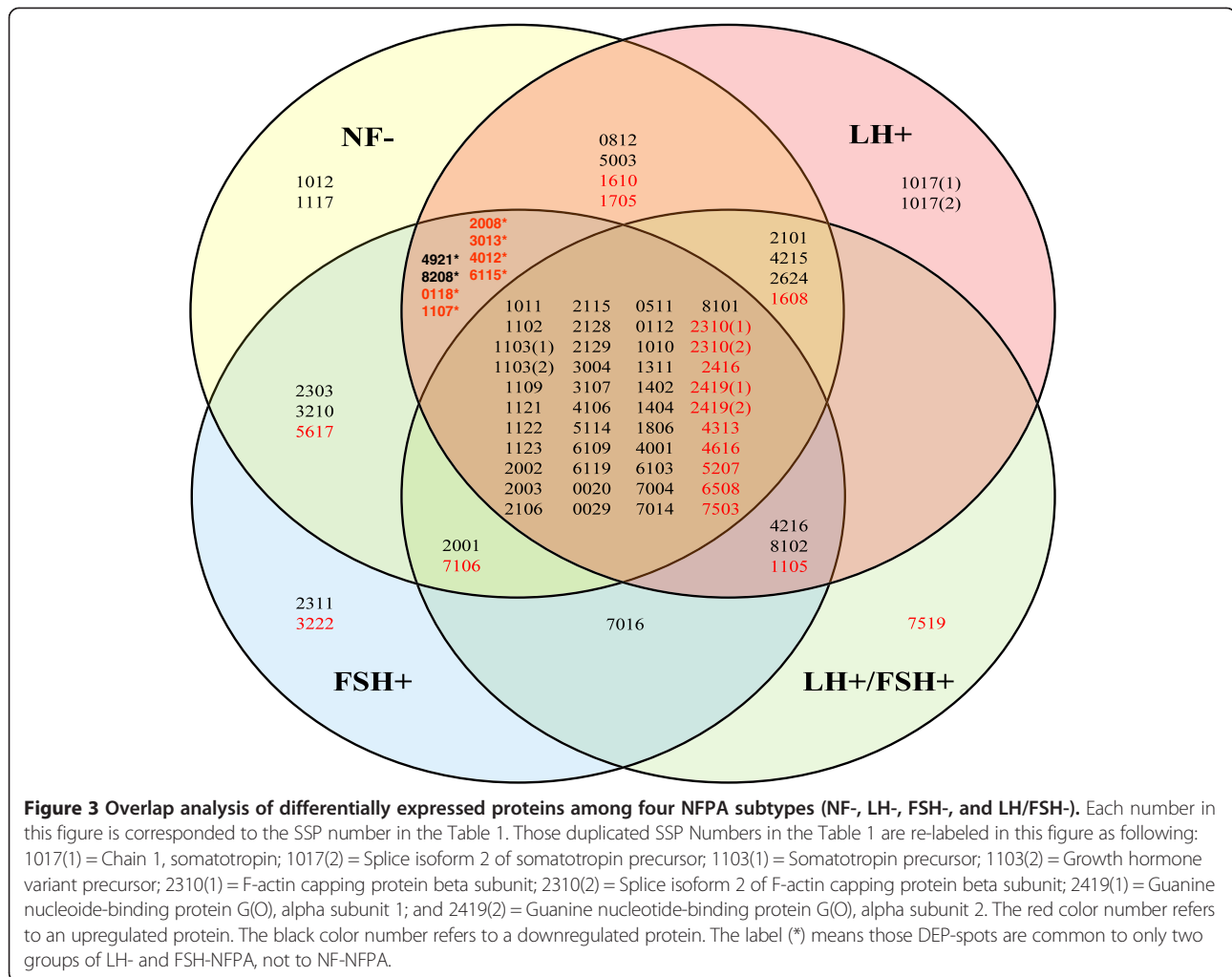
Table 1 Differentially expressed proteins in different subtypes of clinically nonfunctional pituitary adenomas versus controls (Continued)

1311	Secretagogin	O76038	6.6(-)	2.1(-)	2.3(-)	3.4(-)
1402	Mu-crystallin homolog	Q14894	16.3(-)	4.6(-)	2.4(-)	4.6(-)
1404	Chain 1: MIMECAN	P20774	38.0(-)	6.1(-)	9.1(-)	16.2(-)
1806	Tissue transglutaminase	P21980	(--)	17.1(-)	(--)	(--)
2001	CD59 glycoprotein	P13987	9.5(-)		2.4(-)	4.1(-)
2303	Serine/threonine protein phosphatase 2A, 55 kDa regulatory subunit B, alpha isoform	Q00007	8.2(-)		2.6(-)	
2311	L-Myc-1 protooncogene protein	P12524			7.4(-)	
2624	Chain 1: dipeptidyl-peptidase II	Q9UHL4	9.3(-)	2.5(-)		5.3(-)
3210	Heat shock protein 27	P04792	2.4(-)		4.9(-)	
4001	ATP binding protein associated with cell differentiation	O14530	11.4(-)	2.3(-)	2.7(-)	4.4(-)
4921	Chain 1: collagen alpha 2 (VI) chain	P12110		5.3(-)	14.7(-)	
5003	Hemoglobin beta-2 chain	P18988	3.1(-)	2.1(-)		
6103	N6-adenosine-methyltransferase 70 kDa subunit	Q86U44	6.2(-)	6.5(-)	(--)	8.3(-)
7004	Hemoglobin beta unit variant	gi1066765	(--)	176.7(-)	(--)	(--)
7014	Hemoglobin beta-2 chain	P18988	(--)	29.4(-)	28.9(-)	99.4(-)
7016	Hemoglobin alpha-2 chain	P01968			20.2(-)	13.3(-)
8101	Chain 1: insulin-like growth factor binding	P24592	(--)	2.9(-)	20.9(-)	5.0(-)
8102	Chain 1: phospholipid hydroperoxide glutathione peroxidase	P36969		3.9(-)	2.1(-)	14.4(-)
8208	Ig kappa chain V-III region SIE	P01620		4.1(-)	32.5(-)	
0118	Lactoylglutathione lyase	Q04760		9.1(+)	10.2(+)	
1105	Lactoylglutathione lyase	Q04760		6.6(+)	8.3(+)	5.1(+)
1107	NADH-ubiquinone oxidoreductase 23 kDa	O00217		4.9(+)	5.2(+)	
1608	ATP synthase beta chain, mitochondrial precursor	P06576	5.0(+)	3.1(+)		2.8(+)
1610	Vimentin	P08670	5.5(+)	2.6(+)		
1705	Rab GDP dissociation inhibitor alpha	P31150	9.4(+)	5.8(+)		
2008	Enhancer of rudimentary homolog	Q14259		5.0(+)	3.7(+)	
2310	F-actin capping protein beta subunit	P47756	2.7(+)	2.2(+)	6.5(+)	3.0(+)
2310	Splice isoform 2 of F-actin capping protein beta subunit	P47756-2 isoform	2.7(+)	2.2(+)	6.5(+)	3.0(+)
2416	Zinc finger protein 266	Q14584	3.4(+)	2.4(+)	7.3(+)	2.8(+)
2419	Guanine nucleotide-binding protein G(O), alpha subunit 1	P09471	7.3(+)	2.1(+)	9.1(+)	9.5(+)
2419	Guanine nucleotide-binding protein G(O), alpha subunit 2	P29777	7.3(+)	2.1(+)	9.1(+)	9.5(+)
3013	Acyl-CoA-binding protein	P07108		2.7(+)	4.3(+)	
3222	Chain 1: Endoplasmic reticulum protein ERP29	P30040			4.1(+)	

Table 1 Differentially expressed proteins in different subtypes of clinically nonfunctional pituitary adenomas versus controls (Continued)

4012	Cytochrome c oxidase polypeptide VIb	P14854		4.4(+)	8.7(+)	
4313	Aldose reductase	P15121	5.7(+)	9.6(+)	14.6(+)	8.1(+)
4616	Tryptophan 5-hydroxylase (Neuronal tryptophan hydroxylase)	Q8IWU9	10.6(+)	2.1(+)	7.8(+)	8.3(+)
5207	Glutathione S-transferase Mu-2	P28161	2.5(+)	2.8(+)	4.2(+)	2.9(+)
5617	Proto-oncogene tyrosine-protein kinase FYN	P06241	2.8(+)		3.9(+)	
6115	Neuronal protein NP25	Q9UI15		4.9(+)	4.6(+)	
6508	Isocitrate dehydrogenase [NADP] cytoplasmic	O75874	6.1(+)	6.7(+)	8.7(+)	4.4(+)
7503	Peroxisomal acyl-coenzyme A thioester hydrolase 2a	P49753	2.8(+)	2.0(+)	2.2(+)	2.5(+)
7519	Chain 1: matrix metalloproteinase-19	Q99542				3.1(+)
7106	40 kDa peptidyl-prolyl cis-trans isomerase	Q08752	4.3(+)		5.0(+)	5.1(+)

LH-NFPA = NFPA that expressed leuteinizing hormone, or lutropin; FSH-NFPA = NFPA that expressed follicle-stimulating hormone, or follitropin; LH/FSH-NFPA = NFPA that expressed both follicle-stimulating hormone and leuteinizing hormone; NF-NFPA = NFPA that had negative immunohistochemical stains for ACTH, FSH, GH, LH, prolactin, and TSH. Each adenoma was graded blindly by a neuropathologist from 0–4 for intensity of staining for each peptide hormone. (–) = decreased relative to controls; (—) = lost relative to controls; (+) = increased relative to controls; (+/–) = no change relative to controls.



IPA to determine significant pathway networks, canonical pathways, disease biological events, and biological toxicity events and to reveal variations in signaling pathway networks to provide pathway networks, canonical pathways, disease biological events, and biological toxicity events that were common or specific to each NFPA subtype.

Differences in pathway networks

For NF-NFPAs, pathway network analysis of 59 DEPs in NF-NFPAs identified three statistically significant pathway networks that involve NF-NFPA-related DEPs (Figure 4A). Those nodes in the top-half of Figure 4A correspond to molecules (genes; proteins) summarized in the bottom-half of Figure 4A. NF-network 1 functions in cell-to-cell signaling and interaction, hematological system development and function, and immune cell tracking; and includes 35 nodes (genes; proteins). Among those 35 nodes, 18 DEPs (51% of total nodes) were MS-identified. ERK1/2, PRL, APOA1, TGF beta, LDL, NOS, IL12 complex, HSPB1, and YWHAQ play key roles in this network. NF-network 2 functions in cardiovascular system

development and function, organism development, and nervous system development and function; and includes 35 nodes (genes; proteins). Among those 35 nodes, nine DEPs (26% of total nodes) were MS-identified. ERK, GH1, PKA, RAS, Akt, VEGF, MAPK, FYN, p85 (pik3r), PI3K complex, and insulin play key roles in this network. NF-network 3 functions in auditory disease, development disorder, and endocrine system disorders; and includes 35 nodes (genes; proteins). Among those 35 nodes, eight DEPs (23% of total nodes) were MS-identified. UBC, FBXO32, P38 MAPK, NFkB complex, PI3K complex, and PKC play key roles in this network.

For LH-NFPAs, pathway network analysis of 65 DEPs in LH-NFPAs identified three statistically significant pathway networks that involve LH-NFPA-related DEPs (Figure 4B). Those nodes in the top-half of Figure 4B corresponded to molecules (genes; proteins) summarized in the bottom-half of Figure 4B. LH-network 1 functions in cardiovascular system development and function, organism development, and cancer; and includes 35 nodes (genes; proteins). Among those 35 nodes, 16 DEPs (46%

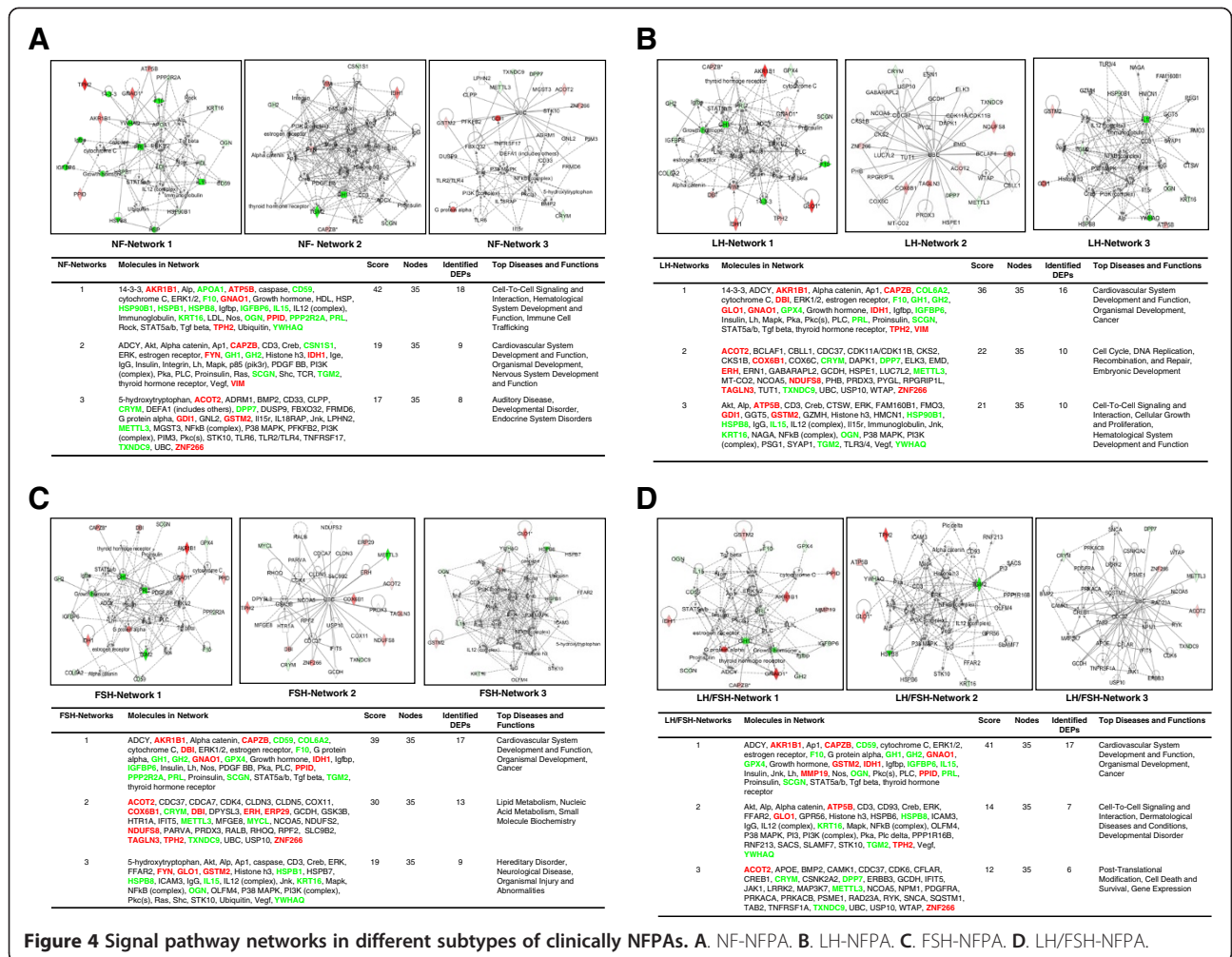


Figure 4 Signal pathway networks in different subtypes of clinically NFPAs. **A.** NF-NFPA. **B.** LH-NFPA. **C.** FSH-NFPA. **D.** LH/FSH-NFPA.

of total nodes) were MS-identified. ERK1/2, PRL, GH1, LH, MAPK, PKC, PKA, 14-3-3, estrogen receptor, TGF beta, and insulin play key roles in this network. LH-network 2 functions in cell cycle, DNA replication, recombination, and repair, embryonic development; and includes 35 nodes (genes; proteins). Among those 35 nodes, 10 DEPs (29% of total nodes) were MS-identified. UBC, CDC37, and COX6B1 play key roles in this network. LH-network 3 functions in cell-to-cell signaling and interaction, cellular growth and proliferation, hematological system development and function; and includes 35 nodes (genes; proteins). Among those 35 nodes, 9 DEPs (26% of total nodes) were MS-identified. P38 MAPK, Akt, ERK, NF-kB complex, CD3, IgG, IL15, IL12 complex, Jnk, VEGF, and TGM2 play key roles in this network.

For FSH-NFPAs, pathway network analysis of 63 DEPs in FSH-NFPAs identified three statistically significant pathway networks that involve FSH-NFPA-related DEPs (Figure 4C). Those nodes in the top-half of Figure 4C corresponded to molecules (genes; proteins) that were summarized in the bottom-half of Figure 4C. FSH-network 1

functions in cardiovascular system development and function, organism development, and cancer; and includes 35 nodes (genes; proteins). Among those 35 nodes, 17 DEPs (49% of total nodes) were MS-identified. ERK1/2, PKA, PLC, TGF beta, TGM2, LH, GH1, PRL, and insulin play key roles in this network. FSH-network 2 functions in lipid metabolism, nucleic acid metabolism, and small-molecule biochemistry; and includes 35 nodes (genes; proteins). Among those 35 nodes, 13 DEPs (37% of total nodes) were MS-identified. UBC, CDC37, and GSK3B play key roles in this network. FSH-network 3 functions in hereditary disorder, neurological disease, organismal injury and abnormalities; and includes 35 nodes (genes; proteins). Among those 35 nodes, 9 DEPs (26% of total nodes) were MS-identified. P38 MAPK, Akt, ERK, NF-kB complex, VEGF, Jnk, MAPK, PI3K complex, Creb, PKC, and HSPB play key roles in this network.

For LH/FSH-NFPAs, pathway network analysis of 55 DEPs in LH/FSH-NFPAs identified three statistically significant pathway networks that involve LH/FSH-NFPA-related DEPs (Figure 4D). Those nodes in the top-half of

Figure 4D corresponded to those molecules (genes; proteins) summarized in the bottom-half of Figure 4D. LH/FSH-network 1 functions in cardiovascular system development and function, organism development, and cancer; and includes 35 nodes (genes; proteins). Among those 35 nodes, 17 DEPs (49% of total nodes) were MS-identified. ERK1/2, Jnk, AP1, NOS, AKR1B1, PRL, LH, PLC, PKC, GH1, STAT5a/b, estrogen receptor, ADCY, and insulin play key roles in this network. LH/FSH-network 2 functions in cell-to-cell signaling and interaction, dermatological diseases and conditions, and development disorders; and includes 35 nodes (genes; proteins). Among those 35 nodes, 7 DEPs (20% of total nodes) were MS-identified. MAPK, TGM2, ERK, NF-kB complex, IL12 complex, VEGF, Creb, Akt, PKA, P38 MAPK, IgG, and CD3 play key roles in this network. LH/FSH-network 3 functions in post-translational modification, cell death and survival, and gene expression; and includes 35 nodes (genes; proteins). Among those 35 nodes, 6 DEPs (17% of total nodes) were MS-identified. UBC, CDC37, SOSTM1, PRKACA, and CREB1 play key roles in this network.

Comprehensive analysis of four sets of pathway networks (Figure 4A-D) revealed: (i) The pathway network (NF-network 2, LH-network 1, FSH-network 1, and LH/FSH-network 1) was highly similar among NF-, LH-, FSH-, and LH/FSH-NFPAs, and functions in cancer, cardiovascular system development and function, organism development, and nervous system development and function; and nodes ERK1/2, GH1, LH, insulin, and PRL play key roles in this common pathway network. However, they are not the same, and display differences among NF-, LH-, FSH- and LH/FSH-NFPAs. (ii) The pathway network (NF-network 1, LH-network 3, and LH/FSH-network 2) is very similar among NF-, LH-, and LH/FSH-NFPAs, and functions in cell-to-cell signaling and interaction, hematological system development and function, immune cell trafficking, cell growth and proliferation, dermatological diseases and conditions, and developmental disorder; network FSH-network 3 is very similar to the above-mentioned three networks, and functions in hereditary disorder, neurological disease, and organism injury and abnormalities. (iii) The network NF-network 3, LH-network 2, FSH-network 2, and LH/FSH-network 3 are basically different, however, they have common nodes UBC and CDC37, and the other nodes are almost different.

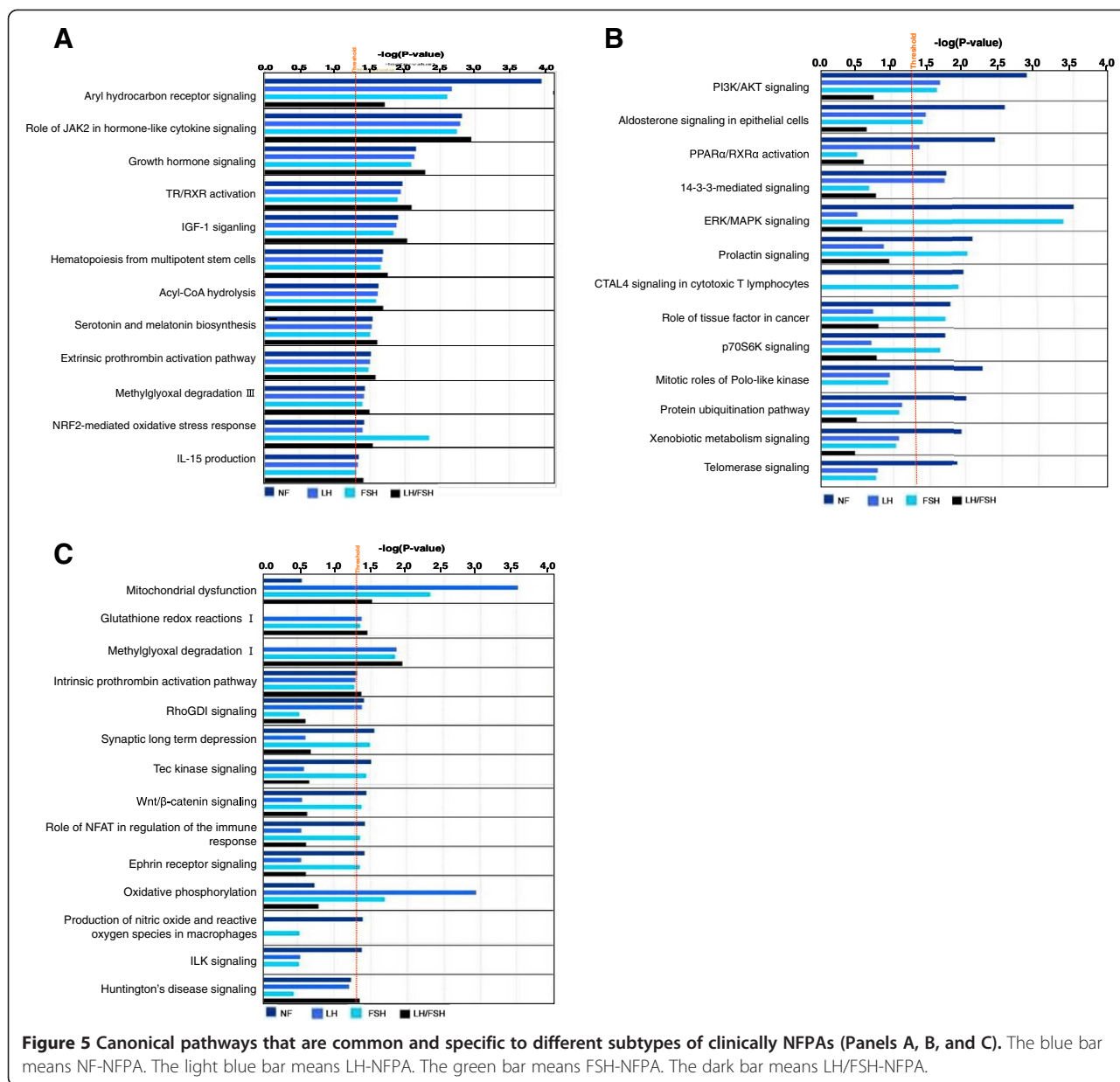
Difference in canonical pathways

Among those DEPs in four NFPA subtypes, pathway network analysis identified 34 statistically significant canonical pathways that involve DEPs in NF-NFPAs, 21 in LH-NFPAs, 28 in FSH-NFPAs, and 18 in LH/FSH-NFPAs. A comparative analysis of those significant canonical pathways was performed among NF-, LH-, FSH-, and LH/

FSH-NFPAs (Figure 5). (i) A total of 12 canonical pathways was common to four NFPA subtypes, including aryl hydrocarbon receptor signaling, role of JAK2 in hormone-like cytokine signaling, growth hormone signaling, TR/RXR activation, IGF-1 signaling, hematopoiesis from multipotent stem cells, acyl-CoA hydrolysis, serotonin and melatonin biosynthesis, extrinsic prothrombin activation pathway, methylglyoxal degradation III, NRF2-mediated oxidative stress response, and IL-15 production (Figure 5A). (ii) Two significant canonical pathways were common to only three NFPA subtypes (NF-, LH-, and FSH-), including PI3K/AKT signaling, and aldosterone signaling in epithelial cells (Figure 5B). (iii) Three significant canonical pathways were common to only three NFPA subtypes (LH-, FSH-, and LH/FSH-), including mitochondrial dysfunction, glutathione redox reactions I, and methylglyoxal degradation I (Figure 5C). (iv) One significant canonical pathway, intrinsic prothrombin activation pathway, was common to only three NFPA subtypes (NF-, LH-, and LH/FSH-) (Figure 5C). (v) Three significant canonical pathways were common to only two NFPA subtypes (NF-, and LH-), including PPAR α /RXR α activation, 14-3-3-mediated signaling, and RhoGDI signaling (Figure 5B and C). (vi) Ten significant canonical pathways were common to only two NFPA subtypes (NF-, and FSH-), including ERK/MAPK signaling, prolactin signaling, CTAL4 signaling in cytotoxic T lymphocytes, role of tissue factor in cancer, p70S6K signaling, synaptic long term depression, Tec kinase signaling, Wnt/ β -catenin signaling, role of NFAT in regulation of the immune response, and Ephrin receptor signaling (Figure 5B and C). (vii) One significant canonical pathway, oxidative phosphorylation, was common to only two NFPA subtypes (LH-, and FSH-) (Figure 5C). (viii) Six significant canonical pathways were specific to only NF-NFPAs, including mitotic roles of Polo-like kinase, protein ubiquitination pathway, xenobiotic metabolism signaling, telomerase signaling, production of nitric oxide and reactive oxygen species in macrophages, and ILK signaling (Figure 5B and C). (ix) One significant canonical pathway, Huntington's disease signaling, was specific to only LH/FSH-NFPAs (Figure 5C).

Differences in disease biological events

Among DEPs in four NFPA subtypes, pathway network analysis identified 77 statistically significant disease biological events that involve in NF-NFPAs, 76 in LH-NFPAs, 76 in FSH-NFPAs, and 79 in LH/FSH-NFPAs. A comparative analysis of those significant disease biological events was performed among NF-, LH-, FSH-, and LH/FSH-NFPAs (Additional file 1: Figure S1). (i) A total of 70 disease biological functional events were common to four NFPA subtypes (NF-, LH-, FSH-, and LH/FSH-) (Additional file 1: Figure S1A-E), including cancer, development and function of cellular, tissue, and multiple organ



systems, morphology of cell, tissue, organ, and tumor, multiple diseases and disorders including inflammatory and neurological diseases, inflammatory and immune responses, cell-to-cell signaling and interaction, cell death and survival, cellular movement, cellular growth and proliferation, protein synthesis, lipid metabolism, molecular transport, cell cycle, carbohydrate metabolism, energy production, vitamin and mineral metabolism, nucleic acid metabolism, DNA replication recombination and repair, amino acid metabolism, drug metabolism, post-translational modification, and behaviors, etc. (ii) Some disease biological events were not common to all NFPA subtypes (Additional file 1: Figure S1F),

including protein degradation, protein folding, protein trafficking, and free radical scavenging, etc.

Difference in biological toxicity events

Among DEPs in four NFPA subtypes, pathway network analysis identified 21 statistically significant biological toxicity events that involve DEPs in NF-NFPAs, 12 in LH-NFPAs, 14 in FSH-NFPAs, and 17 in LH/FSH-NFPAs. A comparative analysis of those significant biological toxicity events was performed among NF-, LH-, FSH-, and LH/FSH-NFPAs (Additional file 1: Figure S2). (i) Ten biological toxicity events were common to four NFPA subtypes (NF-, LH-, FSH-, and LH/FSH-), including cardiac

arrhythmia, liver hypertrophy, renal inflammation, renal nephritis, cardiac pulmonary embolism, cardiac stenosis, increased levels of bilirubin, kidney failure, increased levels of potassium, and glutathione depletion in liver. (ii) Two biological toxicity events were common to only three NFPA subtypes (NF-, FSH-, and LH/FSH-), including increased levels of hematocrit, and increased levels of red blood cells. (iii) Two biological toxicity events were common to only two NFPA subtypes (NF-, and LH/FSH-), including cardiac infraction, and cardiac necrosis/cell death. (iv) One biological toxicity event, liver hyperplasia/hyperproliferation, was common to only two NFPA subtypes (NF-, and LH-). (v) Two biological toxicity events were common to only two NFPA subtypes (NF-, and FSH-), including renal necrosis/cell death, and glomerular injury. (vi) Four biological toxicity events were specific to NF-NFPAs, including cardiac fibrosis, cardiac inflammation, cardiac arteriopathy, and liver cirrhosis. (vii) Three biological toxicity events were specific to LH/FSH-NFPAs, including heart failure, liver necrosis/cell death, and liver damage.

Discussion

Reliability of DEP data is the most-important aspect of 2DGE-based comparative proteomics and for pathway network analysis. In order to achieve reliable DEP data of each NFPA subtype relative to controls, four strategies were applied: (a) spatial and quantitative reproducibility and linear dynamic range of 2DGE analysis systems were optimized and evaluated carefully [32,33]. An appropriate amount (70 μ g) of protein for each 2DGE gel was used, and a 3-fold "cut-off" with statistical significance ($p < 0.05$) was used to determine a DEP. (b) For biological reproducibility, eight tissue samples for controls and three tissue samples for each NFPA subtype were used; and for technique reproducibility, each biological sample was analyzed with 2DGE for 3–5 times. Thus, a total of 30 gel images for controls and 9 gel images for each NFPA subtype was used to detect the DEPs with 3-fold cut-off value ($p < 0.05$) between each NFPA subtype relative to controls (see Figure 2). (c) proteomic heterogeneity of those eight controls was analyzed [34] and used to assist in the determination of DEPs for each NFPA subtype. (d) DEP data were correlated with comparative transcriptomics data, and validated with reverse transcriptase real-time polymerase chain reaction (RT-PCR) [15,35] to validate the DEP data.

In our long-term NFPA proteomics program, we demonstrated DEP profile between NFPAs and controls [15,35], including 50 DEPs (21 up-regulated and 29 down-regulated) contained in 72 2D gel-spots. Those DEPs also correlated with differentially expressed genes (DEGs; $n = 284$) from transcriptomics analysis, and were validated with RT-PCR [15,35]. Moreover, pathway network

analysis of those 50 DEPs [15,35], 111 protein mapping data [11], and 17 nitroproteins [17-19] revealed four important signal pathway networks, including mitochondrial dysfunction, oxidative stress, cell-cycle dysregulation, and MAPK-signaling system abnormality [23]. However, these proteomic studies [15,35] and pathway network analysis [23] did not consider the NFPA heterogeneity, which is an important clinical problem with NFPAs. The differential expressions (NF-, LH-, FSH-, and LH/FSH-positive) of LH and FSH in NFPAs are the common NFPA subtypes.

The present study, for the first time, revealed proteome heterogeneity of four NFPA subtypes (NF-, LH-, FSH-, and LH/FSH-positive). A set of DEP and signaling pathway network data was achieved among four NFPA subtypes. A comprehensive analysis of those complicated DEP data, pathway networks, canonical pathways, disease biological events, and biological toxicity events revealed several signaling pathway systems that were common and specific to different NFPA subtypes and functioned in an NFPA, including MAPK-signaling abnormality, oxidative stress, mitochondrial dysfunction, and cell-cycle dysregulation.

MAPK-signaling abnormality

This common signaling pathway network abnormality occurs among four NFPA subtypes. The biological significance of MAPK-signaling abnormality in a pituitary adenoma has been described [23]. MAPK signaling pathway network involves stimulus (mitogens, cytokines, growth factors, and stress, etc.), G-protein (Cdc42, Ras, Rac, and Rho), MAPKKK (Raf, Tpl2, MEKK, MLK, TAK, ASK, and TAO), MAPKK (MEK), MAPK (ERK, JNK, and p38), and responses (proliferation, differentiation, apoptosis, and migration). ERKs, JNKs, and p38-MAPKs are the three main MAPK subfamilies. ERK 1/2 is activated by MEK1/2, which is activated by Raf, Ras, and growth factors or mitogens; Raf activity, as the main effector of Ras, is suppressed by cyclic AMP-dependent kinase (PKA) in a normal cell. JNKs are activated by MEK4/7, and p38-MAPKs are activated by MEK3/4/6. The upstream signal of MEK3/4/6/7 is from Rac, Rho, cdc42, cytokines, or stresses. NF- κ B, TNF α , and interleukin-1 regulate this pathway system. The details of MAPK signaling pathways in cancer were reviewed [36-38]. MAPK pathways are emerging as potential therapeutic targets for cancer, and development of inhibitors of MAPK pathways is important for cancer therapy. Pathway analysis of DEPs among four NFPA subtypes demonstrated that ERK1/2, ERK, MAPK, GH1, Ras, and NF- κ B were the key nodes in their pathway networks (Figure 4A-D); and the role of JAK2 in hormone-like cytokine signaling, growth hormone signaling, and ERK/MAPK signaling were signaling pathway networks in adenomas. Even though MAPK-signaling abnormalities are a common pathway system

that function in four NFPA subtypes, the MAPK-signaling system is very complicated and includes multiple components, and some differences are present in the MAPK signaling network system among four NFPA subtypes. For example, networks that involve the MAPK-signaling system (Figure 4) are not the same among four NFPA subtypes; and ERK/MAPK signaling of the MAPK-signaling system is statistically significant in only NF- and FSH-NFPAs (Figure 5B).

Oxidative stress (OS)

OS is a common signaling pathway system among four NFPA subtypes. The biological significance of oxidative stress in pituitary adenomas has been described in detail [23]. Many studies indicated the presence of nitric oxide synthase (NOS) in the human and rat pituitaries [39-43], and the increased NOS activities and its increased mRNA have been found in pituitary adenomas relative to controls [43,44]. Nitric oxide (NO) is involved in the hypothalamic-pituitary-adrenocortical axis [45]. NO activates release of luteinizing hormone-releasing hormone (LHRH) and follicle-stimulating hormone-releasing hormone (FSHRH) from the hypothalamus, and of LH and FSH from the pituitary [46-48], stimulates or inhibits the secretion of PRL [49], regulates growth hormone (GH) secretion in the normal human pituitary and in acromegaly [50,51], and modulates GH secretion in a dose-dependent manner in GH adenomatous cells from human pituitary adenomas [52]. Our pathway analysis of DEPs clearly revealed a statistically significant NRF2-mediated oxidative stress response canonical pathway common to each NFPA subtype. However, some differences in the oxidative stress system were found; for example, oxidative phosphorylation was common to only LH- and FSH-NFPAs (Figure 5C); and production of NO and reactive oxygen species in macrophages was specific to LH-NFPAs (Figure 5C).

Mitochondrial dysfunction

This common pathway system occurs among LH-, FSH-, and LH/FSH-NFPAs, except NF-NFPAs (Figure 5C). The biological significance of mitochondrial dysfunction in human pituitary adenoma was described [23]. Mitochondrial dysfunction was confirmed with a mitochondrial morphological change in a pituitary tumor, including an increased number of mitochondria, ultrastructurally abnormal mitochondria, large mitochondria, mitochondrial swelling, and characteristic vesicular mitochondria. Anti-mitochondrial staining showed intense and granular mitochondria, and electron microscopy showed swollen mitochondria in the cytoplasm with featured lamellar cristae in the spindle-cell oncocytophysis of the adenohypophysis. Notable differences in the structure and function of mitochondria appeared between cancer and normal cells, and included differences in mtDNA sequence, molecular composition, and metabolic

activity [53,54]. Mitochondria involve multiple metabolic functions that include oxidative phosphorylation - an energy-generating process that couples oxidation of respiratory substances to ATP synthesis, oxidative decarboxylation of pyruvate, the tricarboxylic acid cycle, fatty-acid oxidation, glycolysis, intracellular homeostasis of inorganic ions such as calcium and phosphate, and intracellular apoptosis [54]. This present study revealed mitochondria-related signaling pathways, including serotonin and melatonin biosynthesis, oxidative phosphorylation, energy metabolism, carbohydrate metabolism, and oxidative stress, that function in human pituitary adenoma cells (Figure 5 and Additional file 1: Figure S1C). Mitochondrial DEPs, including NADH-ubiquinone oxidoreductase 23 kDa and ATP synthase beta chain, were identified in NFPAs.

Cell-cycle dysregulation

This dysregulation is a common pathway system among four NFPA subtypes. The biological significance of cell-cycle dysregulation in human pituitary adenomas was described [23] and reviewed [55-58]. The present study clearly demonstrated cell-cycle network (Figure 4B) and cell cycle regulation (Additional file 1: Figure S1F) in NFPAs. DEP data clearly demonstrated that an important cell-cycle regulator, 14-3-3 protein, was down-regulated (NF: lost; LH: lost; FSH: 6.4-fold; and LH/FSH: 15.5-fold) in four NFPA subtypes relative to controls (Table 1). Furthermore, our previous nitroproteomic data demonstrated that a nitrated proteasome could interfere with functions of the ubiquitin-proteasome system in cell-cycle regulation [23]. Also, the present study clearly demonstrated that ubiquitin C (UBC) was the key node among four NFPA subtypes (Figure 4) to suggest that oxidative/nitrative stress might also be involved in cell-cycle dysregulation in human pituitary adenomas.

In summary, although those pathway systems are common to four NFPA subtypes, one must note that those pathway network systems are, in fact, different among four NFPA subtypes. First, most nodes had different expression levels among four NFPA subtypes - with strong evidence of those DEP data in Table 1 and Figure 3. Second, those pathway networks were not completely the same among four NFPA subtypes - with evidence in Figures 4 and 5. Third, the main pituitary hormones, growth hormone and prolactin, clearly demonstrated multiple isoforms, and were differentially expressed in four NFPA subtypes relative to controls (Table 1). Those abnormal expressions of those pituitary hormones significantly functioned in pathway systems such as MAPK-signaling system described above (Figures 4 and 5), and were involved in pathophysiological processes. Therefore, those DEP profiles (Table 1 and Figure 3), the functional characteristics of those DEPs, and variations in signaling pathway systems (Figures 4 and 5) provide a heterogeneous profile of

human NFPA proteomes. Such a heterogeneous database is essential for an in-depth understanding of NFPA-proteome heterogeneity to accurately clarify basic NFPA molecular mechanisms and to discover biomarkers for effective diagnosis, therapy, and prognosis to achieve personalized medicine practice for an NFPA.

Conclusions

The present study used large-scale quantitative proteomics and systems biology strategies to clarify variations in proteomes and network systems among four NFPA subtypes and to elucidate NFPA-proteome heterogeneity. Results demonstrate common and specific DEP profiles and pathway networks among four NFPA subtypes and for the first time reveal NFPA-proteome heterogeneity. Those data provide a starting point to discover effective biomarkers and effective targets to achieve personalized

medicine practice for an NFPA. Further experiments and more biological specimens are needed to investigate the biological significance of each altered pathway system in an NFPA biological system.

Methods

Pituitary adenomas, control tissues, and preparation of proteins

Differential gel spots that contained DEPs between different NFPA subtypes versus controls were derived from re-analysis of 2DGE images [15,35] that included eight whole control pituitary tissues and twelve NFPA tissues, and each sample had three to five replicate 2DGE images. Also, DEPs were validated with the proteomic variation data of eight controls [34]. Clinical information of pituitary adenoma and control tissue samples was collected in Table 2. Collection and management of those

Table 2 Clinical information of clinically nonfunctional pituitary adenoma and control pituitary samples

Groups	Sample ID	Sex/Age	Clinical information	Immunohistochemistry
NF-NFPA	T164	M/35	Non-functional, visual loss, 3 × 3.5 × 4 cm. Partial hypopituitarism	Neg.
	T217	M/39	Non-functional	Neg.
	T219	M/68	Non-functional, 1.9 × 2.3 × 2.2 cm, invasion of the right cavernous sinus	Neg.
LH-NFPA	T208	F/47	Non-functional, 2 × 2 × 2 cm	LH 1-2+
	T204	M/47	Non-functional	LH 3+
	T237	F/40	Non-functional, right cavernous sinus extension	LH 2+
FSH-NFPA	T57	F/59	Non-functional, 2 × 3 cm	FSH 1+
	T89	M/62	Non-functional, 2 × 2.3 × 2.3 cm	FSH 2+
	T77	M/67	Non-functional, 2 × 2.2 × 2.4 cm, questionable cavernous sinus	FSH 2+
LH/FSH-NFPA	T65	F/54	Non-functional, 4 × 4 × 4 cm, cavernous sinus invasion	LH 2+, FSH 1+
	T138	M/60	Non-functional, 2.9 × 3.1 × 3.5 cm	LH 2+, FSH 2+
	T185	M/66	Non-functional, 2.8 × 2 × 2.4 cm. Bilateral cavernous sinus invasion	LH 2-3+, FSH 2-3+
Control pituitary (Con)	C2	M/27	Black, none	DNT
	C3	F/40	White, Multiple toxic compounds. Blood: HepBb (+), HepC (+), HIV (-)	DNT
	C4	M/45	White, Drowning. Blood alcohol = 3.1 g/L; no other drugs detected. Blood: HepB (+), HepC (+), HIV (-)	DNT
	C5	M/36	White, Multiple toxic materials. Blood alcohol = 0.5 g/L. Blood: HepB (+), HepC (-), HIV (-)	DNT
	C7	F/34	Black, Gunshot wound to chest. Blood alcohol = 0.3 g/L; no drugs. Blood: HepB (+), HepC (-), HIV (-)	DNT
	C8	F	White, 15 h gunshot wound to head. No drugs or alcohol. Blood: HepB (-), HepC (-), HIV (-)	DNT
	C9	M/55	White, 12 h gunshot wound to chest. No alcohol or drugs. Blood: HepB (-), HepC (-), HIV (-)	DNT
	C10	F/47	White, Smoke inhalation. No drugs or alcohol. Numerous amyloids present in brain. Early autolytic changes to brain. Blood: HepB (-), HepC (+), HIV (-)	DNT

Note: All those hormones (ACTH, LH, FSH, PRL, GH, and TSH) were immunohistochemistry-tested in each pituitary adenoma tissue. Neg. = Immunohistochemical stains for ACTH, LH, FSH, PRL, GH, and TSH were negative. LH+ = nonfunctional pituitary adenoma that expressed leuteinizing hormone, or lutropin; FSH+ = nonfunctional pituitary adenoma that expressed follicle-stimulating hormone, or follitropin; FSH+, LH+ = nonfunctional pituitary adenoma that expressed both follicle-stimulating hormone and leuteinizing hormone. Adenomas were graded blindly by a neuropathologist (from 0–4) for the intensity of staining for each peptide hormone. NFPA = nonfunctional pituitary adenoma. DNT = do not test.

tissue samples were approved by the Institutional Review Board (IRB) of the University of Tennessee Health Science Center. The detailed sample collection procedure was described [35]. Each control pituitary tissue (0.45–0.70 g; n = 8) and each NFPA tissue (15–75 mg; n = 12) was homogenized individually, lyophilized, and protein content was quantified; proteins (70 µg) were used for a 2DGE analysis. The detailed procedure of protein sample preparation was described [11].

2DGE and 2D gel image analysis

First-dimension, IEF, was carried out on a Multiphor II instrument (GE Health) with 70 µg protein sample and precast IPG strips (pH 3–10 NL; 180 × 3 × 0.5 mm). After equilibration of IEF-separated proteins, second-dimension, SDS-PAGE, was carried out with a 12% PAGE resolving gel (190 × 205 × 1.0 mm) in a vertical PROTEAN plus Dodeca™ Cell (Bio-Rad) which can analyze up to 12 gels at a time. 2DGE-separated proteins were visualized with a modified silver-staining method. Silver-stained 2DGE gels were digitized and analyzed with a PDQuest system (Version 7.1.0; Bio-Rad). A matched analysis set that contained 30 gel images from 8 control pituitary samples, 9 gel images from 3 NF-NFPA samples, 9 gel images from 3 LH-NFPA samples, 9 gel images from 3 FSH-NFPA samples, and 9 gel images from 3 LH/FSH-NFPA samples (a control pituitary as master gel) used to compare each DEP of NF-, LH-, FSH-, and LH/FSH-NFPAs relative to controls, respectively. Comparative analyses were carried out with the mean normalized volume between each NFPA subtype and controls. The “cutoff point” value for a significant difference of a differential spot was a three-fold difference. The detailed 2DGE method and 2D gel image analysis were described [11].

MALDI-TOF PMF and LC-ESI-MS/MS analyses

Each 2D gel-spot that contained a DEP was excised. Protein was subjected to in-gel digestion with trypsin, purification of tryptic peptides with a Zip-TipC18 micro-column, followed by analysis with a Perseptive Biosystems MALDI-TOF Voyager DE-RP mass spectrometer (Framingham, MA, USA) and with an LCQ^{Deca} mass spectrometer (LC-ESI-Q-IT) equipped with a standard electrospray source (ThermoFinnigan, San Jose, CA, USA). For MALDI-TOF MS, peptide mass fingerprint (PMF) data were generated; PMF data were used to identify protein with a search of the UniProt database with search software Peptide-Ident (<http://us.expasy.org/tools/peptident.html>) and Mascot (<http://www.Matrixscience.com>). For LC-ESI-Q-IT MS, tandem mass spectrometry (MS/MS) data were generated; MS/MS data were used to identify protein with a search of the UniProt and NCBI nr databases with the

SEQUEST software. Detailed experimental procedures were described [11].

Pathway network analysis

The Ingenuity Pathway Analysis (IPA) system was used to obtain cellular pathways that might be modified by protein changes identified in these experiments. IPA automatically generated networks of gene, protein, small-molecule, drug, and disease associations on the basis of “hand-curated” data held in a proprietary database. Identifiers (Swiss-Prot identification number) of DEPs were uploaded as an Excel spreadsheet file into the Ingenuity software (Ingenuity Systems, Redwood City, CA, USA). Each human identification number was mapped to its corresponding molecule in the Ingenuity Pathway Knowledge Base. Biological functions assigned to each network were ranked according to significance of that biological function to the network. Protein networks were algorithmically generated based on their connectivity and were assigned a score. The score was used to rank networks according to how relevant they were to the proteins in the input data set. The network was presented as a graph that indicated the molecular relationship between proteins.

Additional file

Additional file 1: Figure S1. Significant disease biological events that are common and specific to different subtypes of clinically NFPAs. The blue bar means NF-NFPA. The light blue bar means LH-NFPA. The green bar means FSH-NFPA. The dark bar means LH/FSH-NFPA. **Figure S2.** Significant biological toxicity events that are common and specific to different subtypes of clinically NFPAs. The blue bar means NF-NFPA. The light blue bar means LH-NFPA. The green bar means FSH-NFPA. The dark bar means LH/FSH-NFPA.

Abbreviations

ACTH: Adrenocorticotrophic hormone; CHAPS: 3-(3-cholamidopropyl) dimethylammonio-1-propanesulfonate; Con: Control pituitary; DEP: Differentially expressed protein; DTT: Dithiothreitol; ERK: Extracellular signal-regulated kinase; ESI: Electrospray ionization; FPA: Functional pituitary adenoma; FSH: Follicle-stimulating hormone; GH: Growth hormone; IEF: Isoelectric focusing; IPA: Ingenuity Pathway Analysis; IPG: Immobilized pH gradient; LC: Liquid chromatography; LH: Luteinizing hormone; MALDI: Matrix-assisted laser desorption ionization; MAPK: Mitogen activated protein kinase; MS/MS: Tandem mass spectrometry; NF: Negative hormone expression; NFPA: Nonfunctional pituitary adenoma; PMF: Peptide mass fingerprint; SDS-PAGE: Sodium dodecyl sulfate–polyacrylamide gel electrophoresis; 2DGE: Two-dimensional gel electrophoresis; TEMED: Tetramethyl ethylenediamine; TOF: Time-of-flight.

Competing interests

The authors declared that they have no competing interests.

Authors' contributions

XZ conceived the concept, designed the entire manuscript, collected data, analyzed data, wrote and revised manuscript, proof read final manuscript, and was responsible for its financial supports and the corresponding works. XW participated in the design, data analysis, preparation of most figures and tables, and edition of manuscript format. YL participated in data analysis and partial figure preparation. DMD participated in the collection of sample and data and critically revised the manuscript. All authors read and approved the final manuscript.

Acknowledgements

The authors acknowledge the financial supports from China "863" Plan Project (Grant No. 2014AA020610-1 to X. Z.), the Xiangya Hospital Funds for Talent Introduction (to X.Z.), the National Natural Science Foundation of China (Grant No. 81272798 to X.Z.), and the Hunan Provincial Natural Science Foundation of China (Grant No. 14JJ7008 to X. Z.), and Ingenuity for the Ingenuity Pathway Analysis free-trial program, and the constructed canonical pathways.

Author details

¹Key Laboratory of Cancer Proteomics of Chinese Ministry of Health, Xiangya Hospital, Central South University, 87 Xiangya Road, Changsha, Hunan 410008, P. R. China. ²Hunan Engineering Laboratory for Structural Biology and Drug Design, Xiangya Hospital, Central South University, 87 Xiangya Road, Changsha, Hunan 410008, P. R. China. ³State Local Joint Engineering Laboratory for Anticancer Drugs, Xiangya Hospital, Central South University, 87 Xiangya Road, Changsha, Hunan 410008, P. R. China. ⁴The State Key Laboratory of Medical Genetics, Central South University, 88 Xiangya Road, Changsha, Hunan 410008, P. R. China. ⁵The Charles B. Stout Neuroscience Mass Spectrometry Laboratory, Department of Neurology, College of Medicine, University of Tennessee Health Science Center, 847 Monroe Avenue, Memphis, TN 38163, USA.

Received: 3 October 2014 Accepted: 11 December 2014

Published online: 24 December 2014

References

- Melmed S: Pathogenesis of pituitary tumors. *Nat Rev Endocrinol* 2011, 7(5):257–266.
- Farrell WE: Pituitary tumours: findings from whole genome analyses. *Endocr Relat Cancer* 2006, 13(3):707–716.
- Zhan X, Desiderio DM: Comparative proteomics analysis of human pituitary adenomas: Current status and future perspectives. *Mass Spectrom Rev* 2005, 24(6):783–813.
- Zhan X, Wang X, Desiderio DM: Pituitary adenoma nitroproteomics: current status and perspectives. *Oxid Med Cell Longev* 2013, 2013:580710.
- Zhan X, Wang X, Desiderio DM: Mass spectrometry analysis of nitrotyrosine-containing proteins. *Mass Spectrom Rev* 2013. doi:10.1002/mas.21413.
- Zhou KY, Jin HH, Bai ZQ, Liu CB: Pituitary adenoma biomarkers identified using proteomic fingerprint technology. *Asian Pac J Cancer Prev* 2012, 13(8):4093–4095.
- Hu X, Zhang P, Shang A, Li Q, Xia Y, Jia G, Liu W, Xiao X, He D: A primary proteomic analysis of serum from patients with nonfunctioning pituitary adenoma. *J Int Med Res* 2012, 40(1):95–104.
- Cruz-Topete D, Christensen B, Sackmann-Sala L, Okada S, Jorgensen JO, Kopchick JJ: Serum proteome changes in acromegalic patients following transphenoidal surgery: novel biomarkers of disease activity. *Eur J Endocrinol* 2011, 164(2):157–167.
- Strathmann FG, Borlee G, Born DE, Gonzalez-Cuyar LF, Huber BR, Baird GS: Multiplex immunoassays of peptide hormones extracted from formalin-fixed, paraffin-embedded tissue accurately subclassify pituitary adenomas. *Clin Chem* 2012, 58(2):366–374.
- Galland F, Chanson P: Classification and pathophysiology of pituitary adenomas. *Bull Acad Natl Med* 2009, 193(7):1543–1556.
- Zhan X, Desiderio DM: A reference map of a pituitary adenoma proteome. *Proteomics* 2003, 3(5):699–713.
- Zhao Y, Giorgianni F, Desiderio DM, Fang B, Beranova-Giorgianni S: Toward a global analysis of the human pituitary proteome by multiple gel-based technology. *Anal Chem* 2005, 77(16):5324–5331.
- Giorgianni F, Desiderio DM, Beranova-Giorgianni S: Proteome analysis using isoelectric focusing in immobilized pH gradient gels followed by mass spectrometry. *Electrophoresis* 2003, 24(1–2):253–259.
- Beranova-Giorgianni S, Giorgianni F, Desiderio DM: Analysis of the proteome in the human pituitary. *Proteomics* 2002, 2(5):534–542.
- Moreno CS, Evans CO, Zhan X, Okor M, Desiderio DM, Oyesiku NM: Novel molecular signaling in human clinically non-functional pituitary adenomas identified by gene expression profiling and proteomic analyses. *Cancer Res* 2005, 65(22):10214–10222.
- Zhan X, Desiderio DM, Wang X, Zhan X, Guo T, Li M, Peng F, Chen X, Yang H, Zhang P, Li X, Chen Z: Identification of the proteomic variations of invasive relative to noninvasive nonfunctional pituitary adenomas. *Electrophoresis* 2014, 35(15):2184–2194.
- Zhan X, Desiderio DM: The human pituitary nitroproteome: detection of nitrotyrosyl-proteins with two-dimensional Western blotting, and amino acid sequence determination with mass spectrometry. *Biochem Biophys Res Commun* 2004, 325(4):1180–1186.
- Zhan X, Desiderio DM: Nitroproteins from a human pituitary adenoma tissue discovered with a nitrotyrosine affinity column and tandem mass spectrometry. *Anal Biochem* 2006, 354(2):279–289.
- Zhan X, Desiderio DM: Linear ion-trap mass spectrometric characterization of human pituitary nitrotyrosine-containing proteins. *Int J Mass Spectrom* 2007, 259(1):96–104.
- Giorgianni F, Beranova-Giorgianni S, Desiderio DM: Identification and characterization of phosphorylated proteins in the human pituitary. *Poteomics* 2004, 4(3):587–598.
- Beranova-Giorgianni S, Zhao Y, Desiderio DM, Giorgianni F: Phosphoproteomic analysis of the human pituitary. *Pituitary* 2006, 9(2):109–120.
- Zhan X, Giorgianni F, Desiderio DM: Proteomics analysis of growth hormone isoforms in the human pituitary. *Proteomics* 2005, 5(5):1228–1241.
- Zhan X, Desiderio DM: Signal pathway networks mined from human pituitary adenoma proteomics data. *BMC Med Genomics* 2010, 3:13.
- Ribeiro-Oliveira A Jr, Franchi G, Kola B, Dalino P, Pinheiro SV, Salahuddin N, Musat M, Góth MI, Czirájk S, Hanzély Z, da Silva DA, Paulino E Jr, Grossman AB, Korbonits M: Protein western array analysis in human pituitary tumours: insights and limitations. *Endocr Relat Cancer* 2008, 15(4):1099–1114.
- Liu Y, Zhuang D, Hou R, Li J, Xu G, Song T, Chen L, Yan G, Pang Q, Zhu J: Shotgun proteomic analysis of microdissected postmortem human pituitary using complementary two-dimensional liquid chromatography coupled with tandem mass spectrometer. *Anal Chim Acta* 2011, 688(2):183–190.
- Liu Y, Wu J, Yan G, Hou R, Zhuang D, Chen L, Pang Q, Zhu J: Proteomic analysis of prolactinoma cells by immuno-laser capture microdissection combined with online two-dimensional nano-scale liquid chromatography/mass spectrometry. *Proc Natl Acad Sci U S A* 2010, 8:2.
- Liu Y, Wu J, Liu S, Zhuang D, Wang Y, Shou X, Zhu J: Immuno-laser capture microdissection of frozen prolactinoma sections to prepare proteomic samples. *Colloids Surf B Biointerfaces* 2009, 71(2):187–193.
- Walsh MT, Couldwell WT: Symptomatic cystic degeneration of a clinically silent corticotroph tumor of the pituitary gland. *Skull Base* 2010, 20(5):367–370.
- Zhou W, Song Y, Xu H, Zhou K, Zhang W, Chen J, Qin M, Yi H, Gustafsson JA, Yang H, Fan X: In nonfunctional pituitary adenomas, estrogen receptors and slug contribute to development of invasiveness. *J Clin Endocrinol Metab* 2011, 96(8):E1237–E1245.
- Magdeldin S, Enany S, Yoshida Y, Xu B, Zhang Y, Zureena Z, Lokamani I, Yaoita E, Yamamoto T: Basics and recent advances of two dimensional-polyacrylamide gel electrophoresis. *Clin Proteomics* 2014, 11(1):16.
- Webster J, Oxley D: Protein identification by MALDI-TOF mass spectrometry. *Methods Mol Biol* 2012, 800:227–240.
- Zhan X, Desiderio DM: Differences in the spatial and quantitative reproducibility between two second-dimensional gel electrophoresis systems. *Electrophoresis* 2003, 24(11):1834–1846.
- Zhan X, Desiderio DM: Spot volume vs. amount of protein loaded onto a gel: a detailed, statistical comparison of two gel electrophoresis systems. *Electrophoresis* 2003, 24(11):1818–1833.
- Zhan X, Desiderio DM: Heterogeneity analysis of the human pituitary proteome. *Clin Chem* 2003, 49(10):1740–1751.
- Zhan X, Evans CO, Oyesiku NM, Desiderio DM: Proteomics and transcriptomics analyses of secretagogin down-regulation in human non-functional pituitary adenomas. *Pituitary* 2003, 6(4):189–202.
- English JM, Cobb MH: Pharmacological inhibitors of MAPK pathways. *Trends Pharmacol Sci* 2002, 23(1):40–45.
- Johnson GL, Lpadat R: Mitogen-activated protein kinase pathways mediated by ERK, JNK, and p38 protein kinases. *Science* 2002, 298(5600):1911–1912.
- Wada T, Penninger JM: Mitogen-activated protein kinases in apoptosis regulation. *Oncogene* 2004, 23(16):2838–2849.
- Ceccatelli S, Hulting AL, Zhang X, Gustafsson L, Villar M, Hokfelt T: Nitric oxide synthase in the rat anterior pituitary gland and the role of nitric oxide in regulation of LH secretion. *Proc Natl Acad Sci U S A* 1993, 90(23):11292–11296.

40. Ueta Y, Levy A, Powell MP, Lightaman SL, Kinoshita Y, Yokota A, Shibuya I, Yamashita H: **Neuronal nitric oxide synthase gene expression in human pituitary tumours: a possible association with somatotroph adenomas and growth hormone-releasing hormone gene expression.** *Clin Endocrinol (Oxf)* 1998, **49**(1):29–38.
41. Lloyd RV, Jin L, Qian X, Zhang S, Scheithauer BW: **Nitric oxide synthase in the human pituitary gland.** *Am J Pathol* 1995, **146**(1):86–94.
42. Pawlikowski M, Winczyk K, Jaranowska M: **Immunohistochemical demonstration of nitric oxide synthase (NOS) in the normal rat pituitary gland, estrogen-induced rat pituitary tumor and human pituitary adenomas.** *Folia Histochem Cytobiol* 2003, **41**(2):87–90.
43. Kruse A, Broholm H, Rubin I, Schmidt K, Lauritzen M: **Nitric oxide synthase activity in human pituitary adenomas.** *Acta Neurol Scand* 2002, **106**(6):361–366.
44. Vankelecom H, Matthys P, Deneef C: **Inducible nitric oxide synthase in the anterior pituitary gland: induction by interferon- γ in a subpopulation of folliculostellate cells and in an unidentifiable population of nonhormone-secreting cells.** *J Histochem Cytochem* 1997, **45**(6):847–857.
45. Riedel W: **Role of nitric oxide in the control of the hypothalamic-pituitary-adrenocortical axis.** *Z Rheumatol* 2002, **59**:36–42.
46. McCann SM, Haens G, Mastrorandi C, Walczewska A, Karanth S, Rettori V, Yu WH: **The role of nitric oxide (NO) in control of LHRH release that mediates gonadotropin release and sexual behavior.** *Curr Pharm Des* 2003, **9**(5):381–390.
47. McCann SM, Karanth S, Mastrorandi CA, Dees WL, Childs G, Miller B, Sower S, Yu WH: **Control of gonadotropin secretion by follicle-stimulating hormone-releasing factor, luteinizing hormone-releasing hormone, and leptin.** *Arch Med Res* 2001, **32**(6):476–485.
48. Pinilla L, Gonzalez LC, Tena-Sempere M, Bellido C, Aguilar E: **Effects of systemic blockade of nitric oxide synthases on pulsatile LH, prolactin, and GH secretion in adult male rats.** *Horm Res* 2001, **55**(5):229–235.
49. Duvilanski BH, Zambruno C, Seilicovich A, Pisera D, Lasaga M, Diaz MC, Belova N, Rettori V, McCann SM: **Role of nitric oxide in control of prolactin release by the adenohypophysis.** *Proc Natl Acad Sci U S A* 1995, **92**(1):170–174.
50. Pinilla L, Tena-Sempere M, Aguilar E: **Nitric oxide stimulates growth hormone secretion in vitro through a calcium- and cyclic guanosine monophosphate-independent mechanism.** *Horm Res* 1999, **51**(5):242–247.
51. Cuttica CM, Giustil M, Bocca L, Sessarego P, De Martini D, Valenti S, Spaziante R, Giordano G: **Nitric oxide modulates in vivo and in vitro growth hormone release in acromegaly.** *Neuroendocrinol* 1997, **66**(6):426–431.
52. Bocca L, Valenti S, Cuttica CM, Spaziante R, Giordano G, Giusti M: **Nitric oxide biphasically modulates GH secretion in cultured cells of GH-secreting human pituitary adenomas.** *Minerva Endocrinol* 2000, **25**(3–4):55–59.
53. Modica-Napolitano JS, Singh KK: **Mitochondria as targets for detection and treatment of cancer.** *Expert Rev Mol Med* 2002, **4**(9):1–19.
54. Modica-Napolitano JS, Singh KK: **Mitochondrial dysfunction in cancer.** *Mitochondrion* 2004, **4**(5–6):755–762.
55. Musat M, Vax VV, Borboli N, Gueorguiev M, Bonner S, Korbonits M, Grossman AB: **Cell cycle dysregulation in pituitary oncogenesis.** *Front Horm Res* 2004, **32**:34–62.
56. Saeger W: **Proliferation markers and cell cycle inhibitors in pituitary adenomas.** *Front Horm Res* 2004, **32**:110–126.
57. Thakker RV: **Multiple endocrine neoplasia type 1 (MEN1) and type 4 (MEN4).** *Mol Cell Endocrinol* 2014, **386**(1–2):2–15.
58. Melmed S: **Mechanisms for pituitary tumorigenesis: the plastic pituitary.** *J Clin Invest* 2003, **112**(11):1603–1618.

Submit your next manuscript to BioMed Central and take full advantage of:

- Convenient online submission
- Thorough peer review
- No space constraints or color figure charges
- Immediate publication on acceptance
- Inclusion in PubMed, CAS, Scopus and Google Scholar
- Research which is freely available for redistribution

Submit your manuscript at
www.biomedcentral.com/submit

